Journal of King Saud University – Science 31 (2019) 445–451

Contents lists available at ScienceDirect

Journal of King Saud University – Science

journal homepage: www.sciencedirect.com

Original article

Spectral, magnetic, thermal, antioxidant and biological studies on new mixed ligand complexes

Tarun Kumar Pal [a,*], Md. Ashraful Alam [a], Subrata Paul [b], Md. Chanmiya Sheikh [c]

[a] Department of Chemistry, Rajshahi University of Engineering & Technology, Bangladesh
[b] Department of Pharmacy, University of Rajshahi, Bangladesh
[c] Department of Applied Chemistry, Faculty of Engineering, University of Toyama, Japan

ARTICLE INFO

Article history:
Received 4 September 2017
Accepted 17 December 2017
Available online 19 December 2017

Keywords:
Antioxidant
SEM
TGA
FAB-mass spectra
Bis(2,4,4-trimethylpentyl)dithiophosphinic acid

ABSTRACT

In this study, new mixed ligand complexes have been synthesized from bis(2,4,4-trimethylpentyl)dithio phosphinic acid ($C_{16}H_{35}PS_2$) and 1,10-phenanthroline ($C_{12}H_8N_2$) with various metal(II) ions. The molecular formula of the metal complexes were $[Mn(C_{16}H_{34}PS_2)(C_{12}H_8N_2)]$ (**1**), $[Fe(C_{16}H_{34}PS_2)(C_{12}H_8N_2)]$ (**2**), $[Ni(C_{16}H_{34}PS_2)(C_{12}H_8N_2)]$ (**3**), $[Zn(C_{16}H_{34}PS_2)(C_{12}H_8N_2)]$ (**4**) and $[Cd(C_{16}H_{34}PS_2)(C_{12}H_8N_2)]$ (**5**). These complexes have been characterized by various physico-chemical techniques such as melting point, molar conductance, magnetic susceptibility measurements as well as UV–vis, IR, TG and mass spectroscopic analyses. The surface morphology was determined by scanning electron microscope (SEM). The magnetic moment value, color as well as spectral measurements suggested that the geometrical structures of the metal complexes were tetrahedral. The spectral data showed that bis(2,4,4-trimethylpentyl)dithiopho sphinic acid and 1,10-phenanthroline ligands acted as uninegative and neutral bidentate ligand, respectively. They also coordinated with metal(II) ion through two sulfur and two nitrogen atoms. The obtained mixed ligand complexes were more stable in air and highly soluble in common organic solvent. The bioefficacy of ligands and metal complexes have been screened against the test microorganism using agar disc diffusion method. The biological activity results of metal complexes showed that complex **4** displayed potential antibacterial activity against *Clostridium botulinum* as compared to the standard drug, imipenem. The complex **2** and **4** were found to have better scavenging activity against 2,2-diphenyl-1-picrylhydrazyl.

1. Introduction

Bis(2,4,4-trimethylpentyl)dithiophosphinic acid (BDTPA) is the sulfur substitution of organo-phosphorous extracting reagent. Sulfur has lower electronegativity as compared to oxygen. Thus electrons of sulfur atom are more easily shared in the formation of metal-sulfur bond and increase the bond strength. BDTPA has been widely used as reagent for the extraction of trace metals in sample (Pal et al., 2012). 1,10-Phenanthroline (Phen) is an important bidentate chelating ligand. It is also rigid planar, hydrophobic and conjugated heteroaromatic system, that forms more stable complexes with transition metal ions (Zhu and Dai, 2017). Mixed ligand complexes containing nitrogen and sulfur atoms play an important role in biological processes. Biological activities of mixed ligand complex depend on the type of metal ion as well as nature of the ligand (Abu Shamma et al., 2017; Thebo et al., 2017). Mixed ligand complexes containing 1,10-Phenanthroline have a unique role in drug industry and potential applications in various fields (Ekennia et al., 2016; Wang et al., 2016). These complexes were investigated for antitumor (Abu Shamma et al., 2017), anticancer (Tosonian et al., 2013), antifungal (Biswas et al., 2016; Ekennia et al., 2016), antibacterial (Biswas et al., 2016; Ekennia et al., 2016), antioxidant (Biswas et al., 2016), antirheumatics (Abu Shamma et al., 2017), antimycoplasmal (Tabrizi et al., 2016), DNA binding and DNA cleavage activity (Ganeshpandian et al., 2014). A number of metal complexes containing 1,10-Phenanthroline have been used as catalyst for the enantioselective hydrolysis of nitrogen-protected amino acid (Thebo et al., 2017), catalyst for enantioselective reduction of acetophenone, catalyst

* Corresponding author.
E-mail address: tkpchem@ruet.ac.bd (T.K. Pal).
Peer review under responsibility of King Saud University.

Production and hosting by Elsevier

https://doi.org/10.1016/j.jksus.2017.12.010
1018-3647/

for hydrolysis of phosphate ester (Thebo et al., 2017), optical materials and solar cell dyes (Ekennia et al., 2016). Numerous metal complexes with 1,10-phenanthroline as a ligand or mixed with other ligands were reported (Crispini et al., 2017; Zhu and Dai, 2017). As a continuation of research in this area, we report herein the synthesis, characterization and biological study of mixed ligand complexes with bis(2,4,4-trimethylpentyl)dithiophosphinic acid and 1,10-phenanthroline. The mixed ligand complexes were found to have the general formula $[M(C_{16}H_{34}PS_2)(C_{12}H_8N_2)]Cl$ (M = Mn (II), Fe(II), Ni(II), Zn(II) or Cd(II)).

2. Experimental

2.1. Materials and physical measurements

All chemicals were analytical grade reagents from Merck and Sigma Aldrich and used without further purification. IR spectra were recorded on an IR Affinity 1S spectrophotometer, Shimadzu, Japan with samples prepared as KBr pellets. UV–Vis absorption spectra were recorded on a T60 UV–vis spectrophotometer (PG Instruments, UK) programmed with Win5 software, version 5.1. The Mass spectra were obtained on a JEOL-JMS-D300 spectrometer. Thermogravimetric analysis was carried out on a TG 60, Shimadzu, at heating rate of 10 °C min^{-1} from room temperature to 800 °C under nitrogen gas. The percentage of mass loss was recorded against the temperature. Magnetic susceptibility and molar conductance measurements were made on a magnetic susceptibility balance (Sherwood Scientific, UK) and an ECOSCAN CON5 conductivity/temperature meter (Eutech Instruments, Singapore, Serial No. 101886), respectively. Particle size and surface morphology were observed on a JEOL, JSM-6360 LV with energy-diffusive X-ray spectroscopy JEOL, JED-2300.

2.2. General procedure for synthesis of mixed ligand complexes

The appropriate quantity of bis(2,4,4-trimethylpentyl)dithio phosphinic acid (1 mmol, 0.322 g) in absolute ethanol (20 ml) was mixed with ethanolic solution of 1,10-phenanthroline (1 mmol, 0.198 g). Then a hot ethanolic solution of metal(II) chloride (1 mmol, 0.198 g of $MnCl_2{\cdot}4H_20$, 0.235 g of $FeCl_2{\cdot}6H_2O$, 0.238 g of $NiCl_2{\cdot}6H_2O$, 0.136 g of $ZnCl_2$ or 0.228 g of $CdCl_2{\cdot}2.5H_2O$) was added drop wise to the resultant solution. The producing solution was refluxed for 0.5 h whereupon the complex was precipitated. The precipitate was separated by filtration and washed several times with hot ethanol. The complexes were purified by recrystallization from ethanol solution. Finally, pure complexes were dried in vacuum over anhydrous calcium chloride. The purity of the complexes was verified using thin-layer chromatography (TLC).

2.3. DPPH radical scavenging ability

The antioxidant activity of the mixed ligand complex **1**–**5** was determined by DPPH method (Bozin et al., 2006; Tabassam et al., 2013). 2 mL of various concentrations of the samples (31.25, 62.50, 125, 250 and 500 μg) was added to 2 mL of a 0.004% chloroform solution of DPPH. The samples were vortexed and incubated in the dark place for 30 min at room temperature. The absorbance was measured against a blank at 517 nm. Butylated hydroxyl toluene (BHT) was used as a standard for comparison. The assay was carried out in triplicate and the mean was reported. The DPPH radical scavenging activity was calculated by the following equation:

$$\text{DPPH radical scavenging activity}(\%) = [(A_{control} - A_{sample})/A_{control}] \times 100$$

where $A_{control}$ is the absorbance of reaction without sample, and A_{sample} is the absorbance of test sample. Sample concentration providing 50% inhibition (IC_{50}) was calculated from the graph.

2.4. Antibacterial and antifungal screening

The antimicrobial activity of ligands and their mixed ligand complexes was screened against *Sterptococcus pneumoniae* (*S. pneumoniae*), *Bacillus subtilis* (*B. subtilis*), *Staphylococcus aureus* (*S. aureus*), *Staphylococcus epidermidis* (*S. epidermidis*) and *Clostridium botulinum* (*C. botulinum*) bacteria as well as *Candida albicans* (*C. albicans*), *Saccharomyces cerevisiae* (*S. cerevisiae*) and *Aspergillus niger* (*A. niger*) yeasts/fungi species using agar disc diffusion method (Allaka et al., 2016; Nagarjuna et al., 2019). The stock solution (1 mg/mL) of the sample was prepared by dissolving 10 mg of the test compound in 10 mL of chloroform. Control was prepared by solvent instead of stock solution. Sterile media was poured into sterilized Petri dishes and allowed to settle for 15 min. Then 100 μL of microorganism was inoculated on media with the help of micropipette. Later on, the sample was placed on the filter disc. Diameter of filter disc was 4 mm. The Petri dishes were incubated at 37 °C for 24 h in case of bacteria and 48 h at 30 °C for fungal strains. Standard antibacterial drug (imipenem) and antifungal drug (fluconazole) were also screened under similar condition for comparison. In order to clarify any effect of chloroform on the biological screening, separate study was carried out only in chloroform. The zone of inhibition was measured in mm and average zone inhibition was determined. Duplicate data was taken for the calculation of mean inhibition.

3. Results and discussion

3.1. Molar conductivity and nature of species

The molar conductance values of metal complexes were found to be in the range 91–109 ohm^{-1} cm^2 mol^{-1} suggesting 1:1 electrolyte as well as ionic in nature (Table 1), due to the presence of one chloride ion in the outside of coordination sphere (Khalil et al., 2012). Melting point gives primary information about the formation of complex. The higher melting point of the prepared complexes (197–283 °C) as compared to ligand indicating the formation of metal complexes (Olanrewaju et al., 2016; Hasan et al., 2016). The sharp melting point indicated the purity of metal complexes. Mixed ligand complexes were soluble in most common solvents like acetonitrile, chloroform, dichloromethane, DMF and toluene. The experimental physicochemical data of the metal complexes were in good agreement with the proposed structural formula (Fig. 1).

3.2. IR spectra and mode of bonding

The infrared spectra gives important information about the nature of functional groups and binding mode of ligand to metal ion in complex. The characteristic absorption bands in the IR spectra were represented in Table 2. A medium band at 1643 cm^{-1} was attributed to stretching mode of the C═N in 1,10-phenanthroline (Anupama et al., 2017; Mahmoud et al., 2016; Onwudiwe et al., 2016; Qi et al., 2015). This band was shifted to lower frequency (18–23 cm^{-1}) in metal complexes which clearly indicated the coordination of the two nitrogen atoms with metal ion. The new peak in the region 524–545 cm^{-1} can be assigned to asymmetric stretching of M—N in metal complexes proving the coordination of the 1,10-Phenanthroline as bidentate cleating agent (Abu-Khadra et al., 2016; Singh et al., 2016). The bands at 2864–2866 cm^{-1} and 2900–2903 cm^{-1} can be attributed to symmetric and

Table 1
Physical properties of mixed ligand complexes.

Ligand/Complexes	Color	Melting point (±3 °C)	Yield (%)	∧ (ohm^{-1} cm^2 mole^{-1})
BDTPA	Greenish liquid	–	–	–
Phen	Colorless	117	–	–
1	Yellowish-green	278	78	97
2	Yellow	210	56	94
3	Blue	197	62	104
4	White	283	47	109
5	White	276	63	91

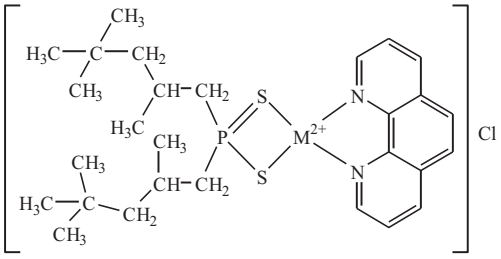

Fig. 1. Proposed structure of metal complexes (**1**–**5**).

asymmetric stretching mode of ν(C—H), respectively (Bal et al., 2014). In metal complexes the characteristic bands of ν(C—H) were almost same, as expected. This further informed that these parts did not participate in coordination. The free bis(2,4,4-trimethylpentyl)dithiophosphinic acid showed a medium band at 2638 cm^{-1} for ν(S—H) vibration (Pal et al., 2010). This band was found to have disappeared in metal complexes, confirming the coordination of sulfur atom with metal ion *via* deprotonation. A medium band of ν(P═S) was observed at 637 cm^{-1} (Pal et al., 2012, 2010; Saglam, 2015). This band was shifted to lower frequency (14–37 cm^{-1}) in metal complexes. In this case, sulfur atom of thiophosphoryl group coordinated with metal ion due to the donation of electrons from sulfur atom to the empty *d*-orbitals of metal ion. In addition, the new peak in the region of 418–426 cm^{-1} was assigned to stretching vibrations of M—S bond (Onwudiwe et al., 2016; Pal et al., 2012) confirming the coordination of sulfur atoms of bis(2,4,4-trimethylpentyl)dithiophosphinic acid with metal ion as uninegative bidentate fashion (Perontsis et al., 2017).

3.3. Electronic spectra and magnetic properties

The electronic spectra provide feasible indication about the ligand arrangement in metal complexes. It also distinguishes among the square-planar, tetrahedral and octahedral geometries of the complexes. Magnetic moment value gives reliable information about paramagnetic or diamagnetic nature and geometry of complex. Color further assists to find out the correct geometry of the complexes (Mahmoud et al., 2017). The ligand (Phen) showed two bands at 265 nm and 295 nm which ascribed to π → π∗ and n → π∗ transition, respectively. BDTPA also displayed two bands at 260 nm and 290 nm which assigned to π → π∗ and n → π∗ transitions, respectively. These bands were shifted towards shorter wavelength region in the spectra of metal complexes which is an evidence of coordination of ligand to metal ions (Ejidike and Ajibade, 2015). The UV–visible spectroscopic data, color and magnetic moment values of the test compounds are listed in Table 3. Complex **1** exhibited one absorption band at 576 nm which assigned to $^6A_1 \rightarrow {}^4T_1$ transition due to tetrahedral geometry. The magnetic moment value and yellowish-green color of the complex are an additional evidence for tetrahedral structure (Siddiqi et al., 2006; Vellaiswamy and Ramaswamy, 2016). The high-spin complex **2** showed a weak band at 530 nm owing to $^5T_2 \rightarrow {}^5E$ transition. In addition, the magnetic moment value as well as yellow color of the complex ascribed for tetrahedral geometry (Iqbal et al., 2013; Nami et al., 2016). The four coordinated complex **3** displayed two peaks at 471 nm and 684 nm, assigned to $^3T_1(F) \rightarrow {}^3T_1(P)$ and $^3T_1(F) \rightarrow {}^3T_2(F)$ transitions. The magnetic moment as well as blue color of the complex are consistent with tetrahedral stereochemistry (Ahmed et al., 2016; Shakdofa et al., 2017). Metal complexes with white color (**4** and **5**) did not show d-d electronic transition due to completely filled d^{10}-orbital (Akter et al., 2017). Furthermore, both complex **4** and **5** exhibited band at 305 nm and 390 nm, respectively (Akter et al., 2017). This band can be assigned to intra ligand charge transfer transition which correspond to tetrahedral geometry (Akter et al., 2017). According to magnetic moment value, complex **1**–**3** were paramagnetic while **2** and **3** were diamagnetic in nature.

3.4. Thermal analysis

Thermogravimetric analysis is a powerful tool to confirm both the composition and stability of the complexes. Table 4 and Fig. 2 represent the proposed chemical change as a function of temperature and corresponding mass loss in each step. 1,10-phenanthroline (Phen) was decomposed progressively in two steps. The first mass loss of Phen occurred in the range of 276–314 °C due to elimination of $0.5O_2$. The second mass loss happened in the range of 315–574 °C due to deduction of $5C_2H_2$ and C_2N_2 species. Thermogravimetry curves showed that the metal complexes were thermally stable up to 180 °C indicating the absence of water molecule inside or outside of coordination sphere (Kianfar et al., 2011). All metal complexes were decomposed pro-

Table 2
Selected infrared absorption frequencies (cm^{-1}) of ligands and their metal complexes.

Ligand/Complexes	ν(C═N)	ν(P═S)	ν(S—H)	ν(M—S) & ν(M—N)
BDTPA	–	637	2638	–
Phen	1643	–	–	–
1	1620	609	–	420 & 540
2	1635	605	–	418 & 524
3	1622	603	–	426 & 545
4	1624	617	–	426 & 524
5	1620	600	–	419 & 528

Table 3
Electronic spectra, magnetic moments and geometry of metal complexes.

Ligand/Complexes	Band (nm)	ε ($Lmol^{-1}cm^{-1}$)	Assignments	μ_{eff} (BM)	Geometry
BDTPA	260	3275	$\pi \rightarrow \pi^*$	–	–
	290	2691	$n \rightarrow \pi^*$		
Phen	265	3081	$\pi \rightarrow \pi^*$	–	–
	295	2863	$n \rightarrow \pi^*$		
1	256	3265	$\pi \rightarrow \pi^*$	5.69	Tetrahedral
	280	3166	$n \rightarrow \pi^*$		
	576	994	$^6A_1 \rightarrow {}^4T_1$		
2	250	3228	$\pi \rightarrow \pi^*$	5.30	Tetrahedral
	282	3154	$n \rightarrow \pi^*$		
	530	335	$^5T_2 \rightarrow {}^5E$		
3	256	3432	$\pi \rightarrow \pi^*$	3.09	Tetrahedral
	285	3331	$n \rightarrow \pi^*$		
	471	539	$^3T_1(F) \rightarrow {}^3T_1(P)$		
	684	350	$^3T_1(F) \rightarrow {}^3T_2(F)$		
4	255	3210	$\pi \rightarrow \pi^*$	Diamagnetic	Tetrahedral
	283	3043	$n \rightarrow \pi^*$		
	305	2538	ILCT		
5	254	3254	$\pi \rightarrow \pi^*$	Diamagnetic	Tetrahedral
	390	1005	ILCT		

Table 4
Thermal data for ligand (Phen) and mixed ligand complexes.

Ligand/Complexes	Temp. (°C)	Mass loss (%)		Leaving species	Residue		
		Theor.	Exp.		Theor. (%)	Exp. (%)	Nature
Phen ($C_{12}H_{10}N_2O$)	276–314	8.08	8.04	$0.5O_2$	–	–	–
	315–574	91.92	91.96	$5C_2H_2$, C_2N_2	–	–	–
(**1**)	298–328	5.92	6.01	$0.5Cl_2$	14.70	14.64	MnS
	329–385	30.29	30.23	$C_{12}H_7N_2$			
	386–716	49.09	49.03	C_2H_2, $7C_2H_4$, pH_3 and H_2S			
(**2**)	182–216	5.91	6.05	$0.5Cl_2$	14.85	14.80	FeS
	217–398	30.24	30.19	$C_{12}H_7N_2$			
	399–658	49.01	48.96	C_2H_2, $7C_2H_4$, pH_3 and H_2S			
(3)	180–210	5.89	6.08	$0.5Cl_2$	15.13	15.07	NiS
	211–327	30.14	30.07	$C_{12}H_7N_2$			
	328–604	48.85	48.78	C_2H_2, $7C_2H_4$, pH_3 and H_2S			
(4)	276–307	5.83	5.84	$0.5Cl_2$	15.97	15.98	ZnS
	308–364	29.84	29.83	$C_{12}H_7N_2$			
	365–678	48.36	48.35	C_2H_2, $7C_2H_4$, pH_3 and H_2S			
(**5**)	271–305	5.38	5.5	$0.5Cl_2$	22.44	22.37	CdS
	306–367	27.54	27.48	$C_{12}H_7N_2$			
	368–726	44.64	44.58	C_2H_2, $7C_2H_4$, pH_3 and H_2S			

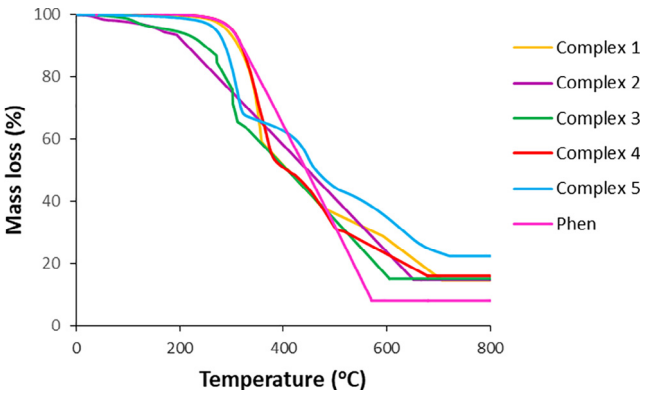

Fig. 2. TG spectrum for the ligand (Phen) and metal complexes (**1**–**5**).

gressively in three steps with almost same trend. In complex **1** the first step occurred in the range of 298–328 °C having mass loss of 6.01% due to the elimination of $0.5Cl_2$ molecule (calcd. 5.92%). The second degradation step happened in the range of 329–385 °C within mass loss of 30.23% (calcd. 30.29%) corresponding to loss of $C_{12}H_7N_2$ species. The third step occurred in the temperature range of 386–716 °C with a mass loss of 49.03% due to the deduction of C_2H_2, $7C_2H_4$, pH_3 and H_2S molecules (calcd. 49.09%). Finally, 14.64% metallic residue remained as MnS (calcd. 14.70%). The first thermal decomposition of complex **2** ensued in the range of 182–216 °C with a mass loss of 6.05% (calcd. 5.91%) due to the elimination of $0.5Cl_2$ molecule. The second step occurred in the range of 217–398 °C with mass loss of 30.19% (calcd. 30.24%) corresponding to the loss of $C_{12}H_7N_2$ moiety. Third step happened due to the loss of C_2H_2, $7C_2H_4$, pH_3 and H_2S molecules with a found mass loss of 48.96% (calcd. 49.01%) in the range of 399–658 °C followed by the formation of 14.80% FeS (calcd. 14.85%). In complex **3** the first mass loss happened in the range of 180–210 °C with mass loss of 6.08% (calcd. 5.89%) corresponding to the deduction of $0.5Cl_2$ molecule. The second step occurred in the range of 211–327 °C due to the loss of $C_{12}H_7N_2$ species with mass loss of 30.07% (calcd. 30.14%). The third step occurred in the range of 328–604 °C with a mass loss of 48.78% (calcd. 48.85%), due to the loss of C_2H_2,

$7C_2H_4$, pH_3 and H_2S molecules, leading finally stable 15.07% NiS as residue (calcd. 15.13%). The first decomposition step of complex **4** occurred in the temperature range of 276–307 °C with mass loss of 5.84% (calcd. 5.83%) corresponding to the loss of $0.5Cl_2$ molecule. Second decomposition step happened in the temperature range of 308–364 °C with mass loss of 29.83% (calcd. 29.84%) due to the elimination of $C_{12}H_7N_2$ species. Third decomposition step occurred in the temperature range of 365–678 °C with mass loss of 48.35% (calcd. 48.36%) corresponding to the loss of C_2H_2, $7C_2H_4$, pH_3 and H_2S molecules leading finally to the most stable species zinc sulphide as residual product (found 15.98%; calcd. 15.97%). The first step of complex **5** occurred in the range of 271–305 °C having mass loss of 5.57% (calcd. 5.38%) due to the elimination of $0.5Cl_2$ molecule. The second degradation step happened in the range of 306–367 °C with mass loss of 27.48% (calcd. 27.54%) corresponding to loss of $C_{12}H_7N_2$ species. The third step occurred in the temperature range of 368–726 °C with a mass loss of 44.58% (calcd. 44.64%), due to the deduction of C_2H_2, $7C_2H_4$, pH_3 and H_2S molecules. Finally, 22.37% (calcd. 22.44%) metallic residue remained as CdS. The experimental molecular mass of metal complexes were in good agreement with suggested molecular formula.

3.5. FAB-mass spectra

The data of mass spectroscopic analysis are presented in Table 5. The molecular ion peak of metal complex **1**–**5** was appeared in the FAB mass spectra at m/z = 591.2, m/z = 592.3, m/z = 593.7, m/z = 600.2 and m/z = 650.2, respectively. However, complex **1**–**5** showed another characteristic peak at m/z = 556.2, m/z = 557.3, m/z = 558.7, m/z = 565.2 and m/z = 615.2, respectively due to the loss of one chloride ligand (Elsayed et al., 2015). Both molecular ion and characteristic peak of metal complexes were in good agreement with their assigned molecular formula. This further confirmed that the mixed ligand complexes were 1:1 ratio as well as mononuclear composition.

3.6. Scanning electron microscope

The surface morphology is one of the characteristics of solid materials. The scanning electron microscope (SEM) was used to evaluate the morphology and particle size of sample. A beam of high-energy electrons of scanning electron microscope creates a variety of signals from the surface of solid matter. These signals provide information about the image of the shape, size of the particles, ductility of substances, strength of materials and how the atoms are arranged in an object. The scanning electron microscope can be as essential tool in metallurgy, forensic science, gemology as well as medical science. From the SEM photographs, the morphology of ligand (Phen) was homogeneously distributed in solid powder. On the other hand, morphology of respective metal complexes was not uniformly distributed and exhibited different structures. The SEM micrographs showed complex **1**, **4** and **5** seemed to be spherical like structure with the particle size approximately 91, 55 and 165 μm, respectively. The complex **2** appeared to have tiny needles with the particle size about 36 μm, while complex **3** indicated cumulated needles like structure.

3.7. Antioxidant activity

Free radicals generate during normal cellular function in body system. Free radicals (such as superoxide anion, hydroxyl radical and hydrogen peroxide) are very reactive. Because of that they interact with proteins, lipids and nucleic acids, may produce various chronic diseases. Therefore, to obstruct the free radical damage in body system, it is important to control drugs that may be rich in antioxidant. Antioxidants have the ability to scavenge free radicals or terminate chain reactions. They play an important role in repairing cellular damage and preventing various human diseases. The scavenging free radical ability of metal complexes is an important property (Ejidike and Ajibade, 2015; Harikishore et al., 2012). Recently to protect the resultant damage, numerous natural as well as synthetic free radical scavengers have been developed and studied (Olanrewaju et al., 2016; Harikishore et al., 2012). The newly synthesized mixed ligand complexes were investigated for their antioxidant properties by DPPH radical scavenging method. 1,1-diphenyl-2-picrylhydrazyl (DPPH) shows a strong absorption band at 517 nm due to its odd electron. An antioxidant reacts with it and produces stable 1,1-diphenyl-2-picrylhydrazine. As a result, the band intensity of DPPH decreases (Asghar et al., 2016). Fig. 3 and Table 6 demonstrate the free radical scavenging activity of metal

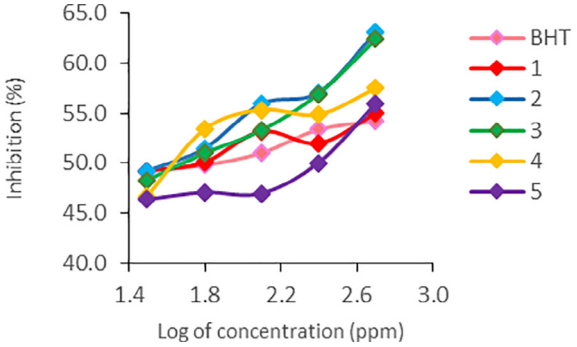

Fig. 3. Antioxidant activity of metal complexes (**1**–**5**).

Table 5
Characteristic peaks of FAB-Mas spectra for mixed ligand complexes.

Complexes					
	1	**2**	3	**4**	**5**
M^+	591.2	592.3	593.7	600.2	650.2
$[M-Cl]^+$	556.2	557.3	558.7	565.2	615.2

Table 6
DPPH free radical scavenging activity of metal complexes.

Compounds						
	1	**2**	**3**	**4**	**5**	BHT
IC_{50} (ppm)	1.67	1.61	1.71	1.63	2.19	1.75
R^2	0.832	0.960	0.968	0.791	0.768	0.958

R^2: correlation coefficient.

Table 7
Antimicrobial activity of the mixed ligand complexes.

Complex No./Standard	Zone of inhibition (mm) against bacteria					Zone of inhibition (mm) against yeasts/fungi		
	S. pneumoniae	*B. subtilis*	*S. aureus*	*S. epidermidis*	*C. botulinum*	*C. albicans*	*S. cerevisiae*	*A. niger*
1	07	10	14	08	09	–	–	–
2	17	11	18	10	07	–	–	–
3	13	09	11	07	11	–	07	13
4	20	13	19	13	22	12	07	15
5	09	07	14	10	12	–	–	–
Imipenem	29	26	28	25	28	–	–	–
Fluconazole	–	–	–	–	–	14	12	17

complexes and BHT. The decreasing absorbance as well as the lower IC_{50} value indicated the higher antioxidant activity of test compounds (Tuyen et al., 2017; Wright et al., 2017). The IC_{50} value of test compounds in descending order was **5** > BHT > **3** > **1** > **4** > **2**. The free radical scavenging activity of complex **3** was lower than that of others, but better than standard antioxidant (BHT). Complex **5** showed very poor scavenging activity. Moreover, complex **2** and **4** were found to have better scavenging activity as compared to the standard antioxidant.

3.8. Antibacterial and antifungal activity

The antimicrobial activity of the complexes are presented in Table 7. Both bis(2,4,4-trimethylpentyl)dithiophosphinic acid and 1, 10-phenanthroline ligands did not show any activity against test microorganisms. Complex **2** and **4** showed an overall good activity against *Sterptococcus pneumoniae* and *Staphylococcus aureus.* The remaining complexes showed very low activity against all bacterial strains. In addition, complex **4** displayed strong antibacterial activity against *Clostridium botulinum* as compared to standard drug, imipenem. On the other hand, complex **3** showed strong activity against *Aspergillus niger.* Complex **4** also exhibited promising activity against *Candida albicans and Aspergillus niger* as compared to standard drug, fluconazole. The biological activity of metal complexes depend on the molecular structure, number of chelate rings, polarity of metal complexes, etc. Only lipid soluble substances can pass through the lipid membrane of microorganism. In the present study some mixed ligand complexes showed less activity due to the lower lipophilicity of the complexes. Because of that the metal complexes could neither block nor inhibit the growth of the microorganisms. While some mixed ligand complexes displayed greater activity than ligands. The increasing activity of mixed ligand complexes can be explained by chelation theory (Mahmoud et al., 2017). The lipophilic nature increased in mixed ligand complexes due to chelation. Therefore, the chelation could increase the ability of metal complex to penetrate through the lipid membrane of test microorganism.

4. Conclusions

In this paper five new mixed ligand complexes have been successfully synthesized and characterized by various physicochemical techniques. Based on the experimental data the bis(2,4,4-trimethylpentyl)dithiophosphinic acid acted as uninegative bidentate ligand. All complexes showed 1:1 electrolyte in nature. Magnetic moment, color, UV–vis spectral, mass and TG observation suggested tetrahedral geometry of all metal complexes. Thermally the mixed ligand complexes were highly stable. Moreover, complex **4** showed strong antibacterial activity against *Clostridium botulinum.*

Acknowledgements

First author would like to thank Ranjit Kumar Biswas, Professor, Department of Applied Chemistry & Chemical Engineering, University of Rajshahi, Bangladesh for providing bis(2,4,4-trimethylpentyl)dithiophosphinic acid. Author also gratefully acknowledges Md. Chanmiya Sheikh for SEM, TG and mass analysis and Dr. Moni Krishna Mohanta (Department of Zoology, University of Rajshahi, Bangladesh) and Subrata Paul for providing the facilities to perform antimicrobial assay.

Appendix A. Supplementary data

Supplementary data associated with this article can be found, in the online version, at https://doi.org/10.1016/j.jksus.2017.12.010.

References

Abu Shamma, A., Abu Ali, H., Kamel, S., 2017. Synthesis, characterization and biological properties of mixed ligand complexes of cobalt(II/III) valproate with 2,9-dimethyl-1,10-phenanthroline and 1,10-phenanthroline. Appl. Organomet. Chem. 1–12. https://doi.org/10.1002/aoc.3904.

Abu-Khadra, A.S., Farag, R.S., Abdel-Hady, A.E.-D.M., 2016. Synthesis, characterization and antimicrobial activity of schiff Base (E)-N-(4-(2-hydroxybenzylideneamino) phenylsulfonyl) acetamide metal complexes. Am. J. Anal. Chem. 7, 233–245.

Ahmed, A.H., Hassan, A.M., Gumaa, H.A., Mohamed, B.H., Eraky, A.M., 2016. Nickel (II)-oxaloyldihydrazone complexes : characterization, indirect band gap energy and antimicrobial evaluation. Cogent Chem. 791, 1–14.

Akter, J., Hanif, A., Islam, M.S., Haque, M., Lee, S.H., Banu, L.A., 2017. Synthesis, characterization and antimicrobial activity of mixed ligand complexes of Mn(II) and Zn(II) with phthalic acid or succinic acid and heterocyclic amines. Der Chem. Sin. 8, 166–174.

Allaka, T.R., Polkam, N., Rayam, P., Sridhara, J., Garikapati, N.S., Kotapalli, S.S., Ummanni, R., Anireddy, J.S., 2016. Design, synthesis and biological activity evaluation of novel pefloxacin derivatives as potential antibacterial agents. Med. Chem. Res. 25, 977–993.

Anupama, B., Aruna, A., Manga, V., Sivan, S., Sagar, M.V., Chandrashekar, R., 2017. Synthesis, spectral characterization, DNA/protein binding, DNA Cleavage, cytotoxicity, antioxidative and molecular docking studies of Cu(II) complexes containing Schiff base-bpy/Phen ligands. J. Fluoresc. 27, 953–965.

Asghar, F., Badshah, A., Butler, I.S., Tabassum, S., Lal, B., Tahir, M.N., 2016. Synthesis, structural characterization, in vitro bioactivities, interaction with SS-DNA and DFT study of 4-chloro-3-ferrocenylaniline. Inorg. Chim. Acta 442, 46–55.

Bal, S., Bal, S.S., Erener, A., Halipci, H., Akar, S., 2014. Synthesis, thermal stability, electronic features, and antimicrobial activity of phenolic azo dyes and their Ni (II) and Cu(II) complexes. Chem. Pap. 68, 352–361.

Biswas, N., Patra, D., Mondal, B., Drew, M.G.B., Ghosh, T., 2016. Synthesis of mixed-ligand complexes of VO^{2+} and VO^{3+} incorporating hydrazone, 1,10-phenanthroline and 8-hydroxyquinoline. J. Coord. Chem. 69, 318–329.

Bozin, B., Mimica-Dukic, N., Simin, N., Anackov, G., 2006. Characterization of the volatile composition of essential oils of some lamiaceae spices and the antimicrobial and antioxidant activities of the entire oils. J. Agric. Food Chem. 54, 1822–1828.

Crispini, A., Cretu, C., Aparaschivei, D., Andelescu, A.A., Sasca, V., Badea, V., Aiello, I., Szerb, E.I., Costisor, O., 2017. Influence of the counterion on the geometry of Cu (I) and Cu(II) complexes with 1,10-phenanthroline. Acta Inorg. Chim. https://doi.org/10.1016/j.ica.2017.05.064.

Ejidike, I.P., Ajibade, P.A., 2015. Synthesis, characterization, antioxidant and antibacterial studies of some metal(II) complexes of tetradentate Schiff Base

Ligand: (4E)-4-[(2-{(E)-[1-(2,4-dihydroxyphenyl)ethylidene]amino}ethyl) imino]pentan-2-one. Bioinorg. Chem. Appl. 2015, 1–9.
Ekennia, A.C., Onwudiwe, D.C., Osowole, A.A., Olasunkanmi, L.O., Ebenso, E.E., 2016. Synthesis, biological, and quantum chemical studies of Zn(II) and Ni(II) mixed-ligand complexes derived from N,N-disubstituted dithiocarbamate and benzoic acid. J. Chem. 2016, 1–12.
Elsayed, S.A., Butler, I.S., Claude, B.J., Mostafa, S.I., 2015. Synthesis, characterization and anticancer activity of 3-formylchromone benzoylhydrazone metal complexes. Transit. Met. Chem. 40, 179–187.
Ganeshpandian, M., Ramakrishnan, S., Palaniandavar, M., Suresh, E., Riyasdeen, A., Akbarsha, M.A., 2014. Mixed ligand copper(II) complexes of 2,9-dimethyl-1,10-phenanthroline: tridentate 3N primary ligands determine DNA binding and cleavage and cytotoxicity. J. Inorg. Biochem. https://doi.org/10.1016/j.jinorgbio.2014.07.021.
Harikishore, D., Reddy, K., Lee, S., 2012. Synthesis, characterization of thiosemicarb a zone metal complexes and their antioxidant activity in different in vitro model systems. J. Serb. Chem. Soc. 77, 229–240.
Hasan, M.S., Kayesh, R., Begum, F., Rahman, S.M.A., 2016. Transition metal complexes of naproxen: synthesis, characterization, forced degradation studies and analytical method verification. J. Anal. Methods Chem. 2016, 1–10.
Iqbal, M.S., Khurshid, S.J., Muhammad, B., 2013. Anti-inflammatory and selective COX-2 inhibitory activities of metal complexes of Schiff bases derived from aldoses. Med. Chem. Res. 22, 861–868.
Khalil, M.M.H., Ismail, E.H., Mohamed, G.G., Zayed, E.M., Badr, A., 2012. Synthesis and characterization of a novel schiff base metal complexes and their application in determination of iron in different types of natural water. Open J. Inorg. Chem. 2, 13–21.
Kianfar, A.H., Sobhani, V., Dostani, M., Shamsipur, M., Roushani, M., 2011. Synthesis, spectroscopy, electrochemistry and thermal study of vanadyl unsymmetrical Schiff base complexes. Inorg. Chim. Acta 365, 108–112.
Mahmoud, W.H., Mohamed, G.G., Mohamedin, S.Y.A., 2017. Spectroscopic characterization, thermal, antimicrobial and molecular docking studies on nano-size mixed ligand complexes based on sudan III azodye and 1,10-phenanthroline. J. Therm. Anal. Calorim. https://doi.org/10.1007/s10973-017-6482-2.
Mahmoud, M.A., Zaitone, S.A., Ammar, A.M., Sallam, S.A., 2016. Synthesis, structure and antidiabetic activity of chromium(III) complexes of metformin Schiff-bases. J. Mol. Struct. 1108, 60–70.
Nagarjuna, D., Al-rajab, A.J., Sharma, M., Mary, M., Ramachandra, G., Albratty, M., 2019. Chemical constituents, in vitro antibacterial and antifungal activity of *Mentha piperita* L. (peppermint) essential oils. J. King Saud Univ. Sci. 31, 528–533. https://doi.org/10.1016/j.jksus.2017.07.013.
Nami, S.A.A., Ullah, I., Alam, M., Lee, D., Sarikavakli, N., 2016. Synthesis, characterization, molecular docking and biological studies of self assembled transition metal dithiocarbamates of substituted pyrrole-2-carboxaldehyde. J. Photochem. Photobiol. B: Biol. 160, 392–399.
Olanrewaju, Adesoji A., Oni, Tolulope I., Osowole, A.A., 2016. Synthesis, characterization and antioxidant properties of some metal(II) complexes of mixed drugs-vitamin Bx and aspirin. Chem. Res. J. 1, 90–96.
Onwudiwe, D.C., Nthwane, Y.B., Ekennia, A.C., Hosten, E., 2016. Synthesis, characterization and antimicrobial properties of some mixed ligand complexes of Zn(II) dithiocarbamate with different N-donor ligands. Inorg. Chim. Acta 447, 134–141.
Pal, T.K., Alam, M.A., Paul, S.R., 2010. Physico-chemical characterization and biological screening of metal complexes with cyanex 301. J. Bangladesh Acad. Sci. 34, 153–161.
Pal, T.K., Alam, M.A., Islam, M.A.A.A.A., Paul, S.R., 2012. Physico-chemical characterization and biological screening of bis(2,4,4-trimethylpentyl) monothiophosphinic acid complexes. J. Sci. Res. 4, 427–435.
Perontsis, S., Tialiou, A., Hatzidimitriou, A.G., Papadopoulos, A.N., Psomas, G., 2017. Nickel(II)-indomethacin mixed-ligand complexes: synthesis, characterization, antioxidant activity and interaction with DNA and albumins. Polyhedron 138, 258–269.
Qi, X., Ren, N., Zhang, D., Zhang, J., 2015. Synthesis, spectroscopic, thermochemical properties of lanthanide complexes with 3,4-diethoxybenzoic acid and 1,10-phenanthroline. Chem. Res. Chin. Univ. 31, 1039–1045.
Saglam, E.G., 2015. Syntheses and structural studies on some new dithiophosphinato complexes of nickel(II), cobalt(II) and mixed pyridino complexes thereof. Inorg. Chim. Acta 434, 188–197.
Shakdofa, Mohamad M.E., Shtaiwi, Majed H., Morsy, N.M., Rasras, A., 2017. Homotrimetallic transition metal complexes of 2-hydroxy-N′1, N′2, N′3-triphenylpropane-1,2,3-tricarbohydrazide preparation, characterization and microbeside activities. Res. J. Pharm. Biol. Chem. Sci. 8, 723–735.
Siddiqi, K.S., Nami, S.A.A., Chebude, Y., 2006. Template synthesis of symmetrical transition metal dithiocarbamates. J. Braz. Chem. Soc. 17, 107–112.
Singh, K., Thakur, R., Kumar, V., 2016. Co(II), Ni(II), Cu(II), and Zn(II) complexes derived from 4-[{3-(4-bromophenyl)-1-phenyl-1H-pyrazol-4-ylmethylene}-amino]-3-mercapto-6-methyl-5-oxo-1,2,4-triazine. Beni-Suef Univ. J. Basic Appl. Sci. 5, 21–30.
Tabassam, N., Ali, S., Shahzadi, S., Shahid, M., Abbas, M., Khan, Q.M., Sharma, S.K., Qanungo, K., 2013. Synthesis, characterization, semi-empirical quantum-mechanical study and biological activity of organotin(IV) complexes with 2-ethylanilinocarbonylpropenoic acid. Russ. J. Gen. Chem. 83, 2423–2437.
Tabrizi, L., McArdle, P., Ektefan, M., Chiniforoshan, H., 2016. Synthesis, crystal structure, spectroscopic and biological properties of mixed ligand complexes of cadmium(II), cobalt(II) and manganese(II) valproate with 1,10-phenanthroline and imidazole. Inorg. Chim. Acta 439, 138–144.
Thebo, A.A., Nahyoon, N.A., Phulpoto, S.N., Khan, A., Shah, S.A., Ali, S., Thebo, K.H., 2017. Synthesis, characterization and biological evaluation of copper (II) metal complex with 1,10-phenanthroline. Org. Med. Chem. 2, 25–27.
Tosonian, S., Ruiz, C.J., Rios, A., Frias, E., Eichler, J.F., 2013. Synthesis, characterization, and stability of iron(III) complex ions possessing phenanthroline-based ligands. Open J. Inorg. Chem. 13, 7–13.
Tuyen, P., Xuan, T., Khang, D., Ahmad, A., Quan, N., Tu Anh, T., Anh, L., Minh, T., 2017. Phenolic compositions and antioxidant properties in bark, flower, inner skin, kernel and leaf extracts of *Castanea crenata* Sieb. et Zucc. Antioxidants 6, 1–14.
Vellaiswamy, G., Ramaswamy, S., 2016. Synthesis, spectral characterisation and antifungal screening of Mn(II) complex with 4-((2-hydroxynaphthalen-1-ylmethylene). J. Pharm. Chem. Biol. Sci. 4, 153–159.
Wang, A.J., Zhang, H., Gao, J.L., Xuan, X.P., 2016. Four novel metal–organic frameworks based on 3,4,7,8-tetramethyl-1,10-phenanthroline: syntheses, structures, and thermal properties. Russ. J. Coord. Chem. 42, 278–284.
Wright, R., Lee, K., Hyacinth, H., Hibbert, J., Reid, M., Wheatley, A., Asemota, H., 2017. An investigation of the antioxidant capacity in extracts from *Moringa oleifera* plants grown in Jamaica. Plants 6, 1–8.
Zhu, Q.Y., Dai, J., 2017. Main group metal chalcogenidometalates with transition metal complexes of 1,10-phenanthroline and 2,2′-bipyridine. Coord. Chem. Rev. 330, 95–109.